
Chiral Phase Boundary of QCD from the Functional Renormalization Group

Jens Braun

Institut für Theoretische Physik, Philosophenweg 19, 69120 Heidelberg, Germany
jbraun@tphys.uni-heidelberg.de

1 Introduction

Phase transitions in QCD are currently very actively researched. Although most of the attention is focused on the phase transition at finite baryon density and temperature and the expected critical point in the phase diagram [1, 2], there are still challenges even at vanishing density, such as a determination of the order of the phase transition or the flavor dependence of the chiral phase transition temperature [3]. Since lattice QCD simulations have not given final answers to all these questions so far, complementary non-perturbative approaches are indispensable to gain a better understanding of the non-perturbative phenomena.

For our non-perturbative study¹ of the chiral phase boundary of QCD at finite temperature, we use the functional renormalization group (RG) [4, 5, 6, 7, 8], applied to a formulation of QCD in terms of microscopic degrees of freedom given by quarks and gluons. At low temperature and momentum scales, QCD can be described well by effective field theories in terms of ordinary hadronic states. But a hadronic picture is eventually bound to fail at higher temperature and momentum scales, owing to asymptotic freedom. The recent discussion of a strongly interacting high-temperature phase of QCD suggests that a simple description of QCD around and above the phase transition temperature does not exist [9]. In this case, a first-principles description in terms of quarks and gluons is most promising to bridge wide ranges in parameter space.

Here we discuss particular problems which are accessible in a formulation in terms of quark and gluons [10, 11]: first, we present our results for the running of the gauge coupling at finite temperature. Second, we discuss the interplay between gluodynamics and (induced) quark dynamics. Finally, we give results for the chiral phase boundary in the plane of temperature and number of quark flavors, obtained from such an investigation of the quark-gluon dynamics at finite temperature.

The functional RG yields a flow equation for the effective average action Γ_k [7],

¹ Talk given at the 2006 ECT* School "Renormalization Group and Effective Field Theory Approaches to Many-Body Systems", Trento, Italy.

$$\partial_t \Gamma_k = \frac{1}{2} \text{STr} \partial_t R_k (\Gamma_k^{(2)} + R_k)^{-1}, \quad t = \ln \frac{k}{\Lambda}, \quad (1)$$

where Γ_k interpolates between the bare action $\Gamma_{k=\Lambda} = S$ and the full quantum effective action $\Gamma = \Gamma_{k=0}$; $\Gamma_k^{(2)}$ denotes the second functional derivative with respect to the fluctuating field. The regulator function R_k specifies the details of the Wilsonian momentum-shell integrations, such that the flow of Γ_k is dominated by fluctuations with momenta $p^2 \simeq k^2$.

It is impossible to study the flow of the most general effective action, consisting of all operators that are compatible with the symmetries of the theory. Therefore we have to truncate the action to a subset of operators, which is not necessarily finite. Nevertheless, such an approximation of the full theory can also describe reliably non-perturbative physics, provided the relevant degrees of freedom in the form of RG relevant operators are kept in the ansatz for the effective action. This is obviously the most problematic part since it requires a lot of physical insight to make the correct physical choice. A first but highly nontrivial check of a solution to the flow equation is provided by a stability analysis of its RG flow, since insufficient truncations generically exhibit IR instabilities of Landau-pole type.

The IR stability of RG flows can be improved by adjusting the regulator to the spectral flow of $\Gamma_k^{(2)}$ [12, 13, 14]. Doing this, we integrate over shells of eigenvalues of $\Gamma_k^{(2)}$ rather than ordinary canonical momentum shells. In a perturbative language, the use of the spectrally adjusted regulator allows for a resummation of a larger class of diagrams. Such an improvement has been successfully applied to the study of QCD at zero and finite temperature [12, 13, 11] and is the underlying technical ingredient for the results presented below.

In the subsequent sections, we use the exponential regulator [7] of the form $R_k(\Gamma_k^{(2)}) = \Gamma_k^{(2)} / [\exp(\Gamma_k^{(2)} / \mathcal{Z}_k k^2) - 1]$, where \mathcal{Z}_k denotes the wave function renormalization of the fields.

2 Running gauge coupling at finite temperature

In this section, we present our study of the running strong coupling at finite temperature. While an investigation of the running of the coupling is interesting in its own right, we will also show in the subsequent sections that it represents a key ingredient of our study of the chiral phase boundary.

Owing to strong coupling, we cannot expect that low-energy gluodynamics are reliably described by a small number of gluonic operators. On the contrary, infinitely many operators become RG relevant in the low-momentum regime and drive the running of the coupling. We truncate the space of possible action functionals to an *infinite* but still tractable set of operators. For gauge invariance, we apply the background-field formalism as developed in [15, 16] and follow the strategy of [17, 12] for an approximate resolution of the gauge

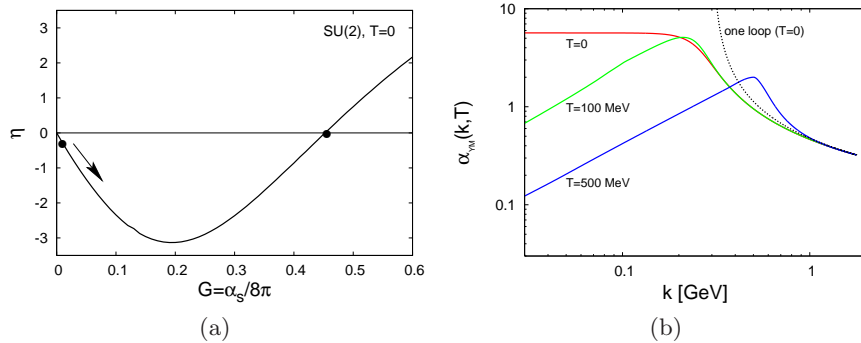


Fig. 1. (a): Anomalous dimension η as a function of $\alpha/8\pi = g^2/32\pi^2$ for $SU(2)$ Yang-Mills theory at vanishing temperature. The anomalous dimension is defined via the background-field wave-function renormalization by $\eta = -\ln \partial_t W_k^{(1)}$. It is related to the flow of the coupling as $\partial_t g_k^2 = \eta g_k^2$. The arrow indicates the RG flow from the initial condition at the UV scale Λ (left dot) to the IR fixed point (right dot). Owing to asymptotic freedom, there exists also a fixed point for $\alpha = 0$. (b): Running $SU(3)$ Yang-Mills coupling $\alpha_{YM}(k, T)$ as a function of k for temperatures $T = 0, 100, 300$ MeV, compared to the one-loop running for vanishing temperature.

constraints [18]. For an introduction to the background-field formalism and to background-field flow equations for gauge theories, we refer the reader to the lecture notes of H. Gies [19]. Apart from standard gauge-fixing and ghost terms, our truncation of the gauge sector consists of an infinite set of operators given by powers of the Yang-Mills Lagrangian,

$$\Gamma_k[A, \bar{\psi}, \psi] = \int_x \mathcal{W}_k(\theta) + \Gamma_k^\psi[A, \bar{\psi}, \psi], \quad \theta = \frac{1}{4} F_{\mu\nu}^a F_{\mu\nu}^a, \quad (2)$$

whereas the quark contributions are summarized in Γ_k^ψ and will be discussed in Sec. 3. For the moment, we restrict our study to the gluonic subspace. Expanding the function $\mathcal{W}_k(\theta) = W_k^{(1)}\theta + \frac{1}{2}W_k^{(2)}\theta^2 + \frac{1}{3!}W_k^{(3)}\theta^3 \dots$, the expansion coefficients span an infinite set of generalized couplings. The background-field method [20] provides us with a non-perturbative definition of the running coupling g_k in terms of the background-field wave function renormalization $W_k^{(1)}$: $g_k^2 W_k^{(1)} = \bar{g}^2$.

Our truncation represents a gradient expansion in the field strength, which includes arbitrarily high gluonic correlators projected onto their small-momentum limit and onto the color and Lorentz structure arising from powers of F^2 . A drawback of such gradient expansions is the appearance of an IR unstable Nielsen-Olesen mode in the spectrum [21]. At finite temperature T , such a mode will be populated by thermal fluctuations, typically spoiling perturbative computations, see e. g. Ref. [22]. Our RG approach allows us to

resolve this problem with the aid of a temperature-dependent regulator which removes the unphysical thermal population of the unstable mode. Thus, we obtain a strictly positive thermal fluctuation spectrum. For details of the implementation of such a regulator, we refer to [11].

Inserting the truncation (2) in the flow equation (1), we find that the running of the coupling is successively driven by all generalized couplings $W_k^{(i)}$. Keeping track of all contributions from the flows of the $W_k^{(i)}$, we obtain a non-perturbative β_{g^2} function in terms of an infinite asymptotic but resumable series in powers of g^2 ,

$$\beta_{g^2} \equiv \partial_t g_k^2 = \sum_{m=1}^{\infty} a_m\left(\frac{T}{k}, N_c\right) \frac{(g^2)^{m+1}}{[2(4\pi)^2]^m}. \quad (3)$$

The coefficients a_m depend on the temperature T and the rank N_c of the gauge group². At vanishing temperature, the β_{g^2} function agrees well with perturbation theory for small coupling. For larger coupling, we find that the integral representation of Eq. (3) has a second zero, corresponding to an IR attractive non-Gaussian fixed point $g_*^2 > 0$, in agreement with the results of Ref. [12], see Fig. 1(a). For an explicit representation of the a_m 's and details of the computation, we refer the reader to Ref. [11]. Note that the appearance of an IR fixed point in Yang-Mills theories is a well-investigated phenomenon in the Landau gauge [25, 26, 27], in accordance with the Kugo-Ojima and Gribov-Zwanziger confinement scenarios [28, 29]. Moreover, it is also compatible with the existence of a mass gap [12] in Yang-Mills theory.

As initial condition for the coupling flow, we use the value of the coupling measured at the τ mass scale [30], $\alpha_s = 0.322$. For scales $k \gg T$, we find agreement with the perturbative running coupling at zero temperature, as one would naively expect. In the IR, the running is strongly modified: The coupling increases towards lower scales until it develops a maximum near $k \sim T$. Below, the coupling decreases according to a power law $g^2 \sim k/T$, see Fig. 1(b). The reason for this behavior can be understood within the RG framework: first, the hard gluonic modes decouple from the RG flow at the scale $k \sim T$. At this point, the wavelength of fluctuations with momenta $p^2 < T^2$ is larger than the extent of the compactified Euclidean time direction. Hence these modes become effectively 3-dimensional and their limiting behavior is governed by the spatial 3d Yang-Mills theory. However, the decoupling of the hard modes alone cannot explain the decrease of the coupling for scales $k < T$. The second ingredient which is needed is the existence of a non-Gaussian IR fixed point also in the reduced 3-dimensional theory. A straightforward matching between

² Odd powers in the coupling g which arise in high-temperature small-coupling expansions [23, 24] are not reproduced in our calculation. This is due to the fact that we have not yet included non-local operators in our truncation. In any case, we do not expect that these operators are quantitatively important for the determination of the chiral phase boundary since, as we will discuss below, chiral symmetry breaking sets in at scales $k < T$.

the $4d$ and $3d$ coupling reveals that the observed power law for the $4d$ coupling is a direct consequence of the strong-coupling IR behavior in the $3d$ theory, $g^2(k \ll T) \approx g_{3d,*}^2 k/T$. Note that this asymptotic behavior can be deduced analytically from the integral representation of Eq. (3), see Ref. [11]. Again, the observed IR behavior at finite temperature is in accordance with recent results in the Landau gauge [31].

3 Chiral Phase Boundary of QCD

For a study of chiral symmetry breaking at finite temperature, we extend our truncation (2) in two directions. To make this more transparent, we divide Γ_k^ψ in Eq. (2) into two terms, $\Gamma_k^\psi = \Gamma_k^{\psi\text{-kin.}} + \Gamma_k^{\psi\text{-int.}}$. With the first term, we include the quark contributions to all gluonic operators, as done in Ref. [32] for QED and in Ref. [11] for QCD:

$$\Gamma_k^{\psi\text{-kin.}}[A, \bar{\psi}, \psi] = \int_x \bar{\psi} \mathcal{D}[A] \psi, \quad (4)$$

where we confine ourselves to massless quarks. An inclusion of mass terms is straightforward and has been done in Refs. [11]. This kinetic term successively contributes to the RG flow of the coupling and accounts for the screening nature of fermionic fluctuations.

The second term, $\Gamma_k^{\psi\text{-int.}}$, accounts for the quark self-interactions. In a consistent and systematic operator expansion, the lowest non-trivial choice for this term is given by³

$$\Gamma_k^{\psi\text{-int.}}[\bar{\psi}, \psi] = \int_x \frac{1}{2} \left[\bar{\lambda}_-(\text{V-A}) + \bar{\lambda}_+(\text{V+A}) + \bar{\lambda}_\sigma(\text{S-P}) \right. \\ \left. + \bar{\lambda}_{\text{VA}}[2(\text{V-A})^{\text{adj}} + (1/N_c)(\text{V-A})] \right]. \quad (5)$$

We have classified the four-fermion interactions according to their color and flavor structure:

$$\begin{aligned} (\text{V-A}) &= (\bar{\psi}\gamma_\mu\psi)^2 + (\bar{\psi}\gamma_\mu\gamma_5\psi)^2, & (\text{V+A}) &= (\bar{\psi}\gamma_\mu\psi)^2 - (\bar{\psi}\gamma_\mu\gamma_5\psi)^2, \\ (\text{S-P}) &= (\bar{\psi}^x\psi^\xi)^2 - (\bar{\psi}^x\gamma_5\psi^\xi)^2, & (\text{V-A})^{\text{adj}} &= (\bar{\psi}\gamma_\mu T^a\psi)^2 + (\bar{\psi}\gamma_\mu\gamma_5 T^a\psi)^2. \end{aligned}$$

Color and flavor singlets are given in the first line. Fundamental color (i, j, \dots) and flavor (χ, ξ, \dots) indices are contracted pairwise. The operators with non-singlet color or flavor structure are given in the second line, where $(\bar{\psi}^x\psi^\xi)^2 \equiv \bar{\psi}^x\psi^\xi\bar{\psi}^\xi\psi^x$, etc., and the $(T^a)_{ij}$ denote the generators of the gauge group in the fundamental representation.

³ Qualitatively, we expect our truncation of the fermionic self-interactions to be reliable for our purposes, since the feed-back of higher-order operators, e. g. $\sim (\bar{\psi}\psi)^4$, is in general suppressed by the one-loop structure of the underlying flow equation.

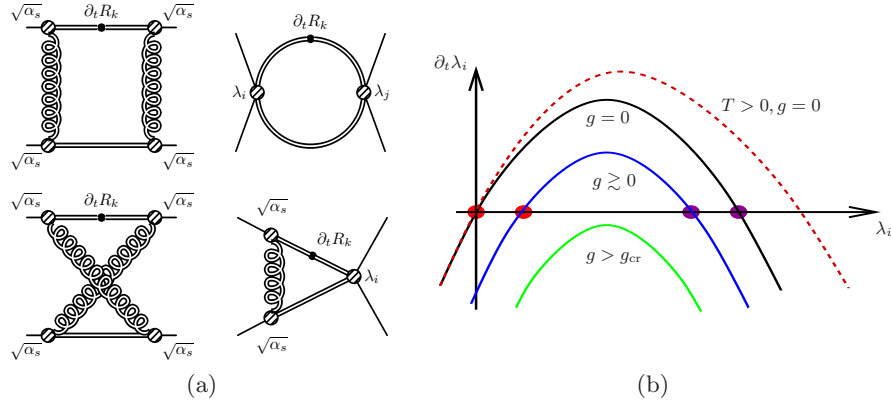


Fig. 2. (a): Representation of the one-particle irreducible (1PI) graphs which are contained in the RG flow equations for the four-fermion interactions. The double-lines represent the fully dressed propagator and the solid black dots denote the insertion of $\partial_t R_k$ in the loop. The four-fermion couplings λ_i are defined in Eq. (5). Note that diagrams with the same topology but with the regulator insertion attached to the other internal lines are present in the RG flow as well. (b): Sketch of a typical β function for the fermionic self-interactions λ_i at vanishing temperature for zero gauge coupling (upper solid curve), for finite gauge coupling $g > 0$ (middle/blue solid curve) and for gauge couplings larger than the critical coupling $g > g_{cr}$ (lower/green solid curve). The effect of finite ratios T/k is illustrated for vanishing gauge coupling by the dashed (red) line.

In the following, we study the four-fermion couplings in the point-like limit, $\lambda_i = \lambda_i(|p_i| \ll k)$. This is a severe approximation in the chirally broken regime where mesons manifest themselves as momentum singularities of the four-fermion couplings. Nevertheless, our point-like truncation can be a reasonable approximation in the chirally symmetric regime⁴. We stress that our truncation (5) for the fermionic self-interactions forms a complete basis, i. e. any other pointlike four-fermion interaction which is invariant under $SU(N_c)$ gauge symmetry and $SU(N_f)_L \times SU(N_f)_R$ flavor symmetry is reducible by means of Fierz transformations. Terms accounting for instantons, as $U_A(1)$ -violating interactions have been neglected as well, since they may become relevant only inside the χ SB regime or for small N_f .

Introducing the dimensionless couplings $\lambda_i = k^2 \bar{\lambda}_i$, the β functions for the four-fermion couplings can be written in the form

$$\partial_t \lambda_i = 2\lambda_i - \lambda_j A_{jk} \lambda_k - b_j \lambda_j g^2 - c_i g^4. \quad (6)$$

Here we use a straightforward finite-temperature generalization of the flow equations for the $\bar{\lambda}_i$, which have been derived and analyzed in [34, 33]. The

⁴ This has recently been quantitatively confirmed for the zero-temperature chiral phase transition in many-flavor QCD [33].

quantities A , b and c are dependent on the ratio T/k , where A is a matrix, and b and c are vectors in the space of λ couplings; see Ref. [11] for an explicit representation of the flow equations. The various terms arising on the RHS of the flow equation of the $\bar{\lambda}_i$ s can be related straightforwardly to one-particle irreducible Feynman-graphs, which are depicted in Fig. 2(a). As initial conditions for the four-fermion couplings, we use $\bar{\lambda}_i \rightarrow 0$ for $k \rightarrow \Lambda \rightarrow \infty$. This choice ensures that the $\bar{\lambda}_i$ are generated solely by quark-gluon dynamics from first principles. This point is very important, as it is contrary to, e.g., the Nambu–Jona-Lasinio model, where the four-fermion couplings serve as independent input parameters.

Our truncation provides a simple picture for the chiral dynamics illustrated by Fig. 2(b): At vanishing gauge coupling, we find fixed points for the four-fermion couplings at $\lambda_i \neq 0$ and $\lambda_i = 0$, where the latter ones are IR attractive. By increasing the gauge coupling g , the RG flow generates quark self-interactions of order $\lambda \sim g^4$, resulting in a shift of the fixed points. Moreover, we observe that the four-fermion couplings approach fixed points λ_* in the IR, if the gauge coupling in the IR remains smaller than a critical value g_{cr} . At these fixed points, QCD remains in the chirally invariant phase. Increasing the gauge coupling beyond the critical coupling $g > g_{\text{cr}}$, the gauge-fluctuation induced λ 's become strong enough to contribute as relevant operators to the RG flow. This is reflected in a destabilization of the IR fixed points [34, 33]. In this case, the four-fermion couplings increase rapidly and approach a divergence at a finite scale $k = k_{\chi\text{SB}}$. Indeed, this strong increase indicates the formation of chiral quark condensates and therefore the onset of chiral symmetry breaking. We recall the NJL model as an illustration: There, the mass parameter m^2 of the bosonic fields in the partially bosonized action is inversely proportional to the four-fermion coupling, $\bar{\lambda} \sim 1/m^2$. In addition, we know from such NJL-type models that their effective action in the bosonized form corresponds to a Ginzburg-Landau effective potential for the order parameter. In its simplest form, the order parameter is given by the expectation value of a scalar field. Symmetry breaking is then reflected in a non-trivial minimum of the this potential. Consequently, the scale $k_{\chi\text{SB}}$ at which the four-fermion couplings diverge is a good measure for the chiral symmetry breaking scale. At this scale, the effective potential for the order parameter becomes flat and starts to develop a nonzero vacuum expectation value.

At this point, we have traced the question of the onset of chiral symmetry breaking back to the strength of the coupling g relative to the critical coupling g_{cr} . At zero temperature, the critical coupling for three colors and not too many (massless) quark flavors is much smaller than the IR fixed point value of the coupling. Therefore QCD exhibits broken chiral symmetry at zero temperature.

At finite temperature, the running of the gauge coupling is strongly modified in the IR. Moreover, the critical coupling becomes larger for increasing ratios T/k . This reflects that the formation of quark condensates require

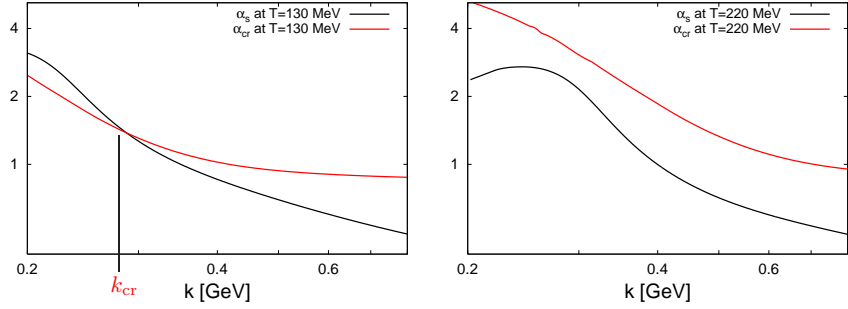


Fig. 3. The figures show the running QCD coupling $\alpha_s(k, T)$ for $N_f = 3$ massless quark flavors and $N_c = 3$ colors and the critical value of the running coupling $\alpha_{\text{cr}}(k, T)$ as a function of k for two values of the temperature, $T = 130$ MeV (left panel) and $T = 220$ MeV (right panel). The existence of the $(\alpha_s, \alpha_{\text{cr}})$ intersection point at the scale k_{cr} in the left panel indicates that the quark dynamics can become critical.

stronger interactions at finite temperatures, since the quarks become stiffer due to the thermal masses.

In Fig. 3, we show the running coupling α_s and its critical value α_{cr} for $T = 130$ MeV and $T = 220$ MeV as a function of the regulator scale k . The intersection point k_{cr} between both gives the scale where the chiral quark dynamics become critical. Above this scale, the system is in the chiral symmetric regime, below it quickly runs into the broken regime. The critical temperature can now be estimated using the lowest temperature for which no intersection point between α_s and α_{cr} exists. We find $T_{\text{cr}} \approx 186$ MeV for $N_f = 2$ and $T_{\text{cr}} \approx 161$ MeV for $N_f = 3$ massless quark flavors in good agreement with lattice simulations [3]. We stress that no other parameter except for the running coupling at the τ mass scale has been used as input for the calculation of the critical temperatures.

Finally, we discuss the chiral phase boundary in the plane of the temperature and number N_f of massless quark flavors computed within our approach, see Fig. 4(a). For small N_f , we observe an almost linear decrease of the critical temperature for increasing N_f with a slope of $\Delta T_{\text{cr}} = T(N_f) - T(N_f + 1) \approx 25$ MeV. Additionally we find the existence of a critical number of quark flavors, $N_f^{\text{cr}} = 12$, above which no chiral phase transition occurs. Since $N_f^{\text{cr}} < N_f^{\text{a.f.}} = \frac{11}{2}N_c = 16.5$, our study confirms the existence of a regime where QCD is chiral symmetric but still asymptotically free. Our value for N_f^{cr} is in agreement with other studies based on the 2-loop β -function [35, 36, 37]. A remarkable feature of the phase boundary is its shape near N_f^{cr} . It is a generic prediction of the IR fixed-point scenario and can be understood from analytic arguments [11]: For $N_f \approx N_f^{\text{cr}}$, where fermionic screening of color charges keeps the coupling small, the coupling must almost reach its maximal

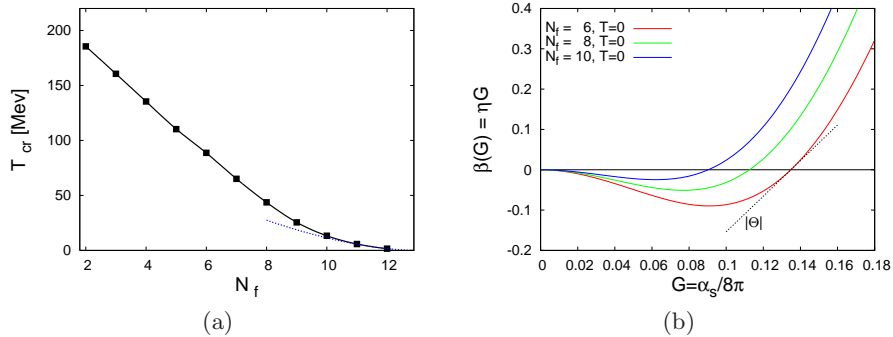


Fig. 4. (a): Chiral phase-transition temperature T_{cr} versus the number of massless quark flavors N_f . The flattening at $N_f \gtrsim 10$ is a consequence of the IR fixed-point structure, see text. The analytic prediction (7) for the phase boundary is depicted by the dashed (blue) line. (b): The figure shows the β function for $N_f = 6, 8, 10$ massless quark flavors (from bottom to top). For illustration, we also show the linear approximation of the β function for $N_f = 6$ whose slope gives the corresponding critical exponent Θ .

value in order to drive the quark sector to criticality. This maximal value can be roughly estimated from the fixed point value g_*^2 of the coupling at zero temperature. In the fixed point regime, the β_{g^2} function is essentially given by the linear term of an expansion around the fixed point, $\beta_{g^2} = -\Theta (g^2 - g_*^2)$, where Θ denotes the *universal* critical exponent. For illustration, we show the β_{g^2} functions for $N_f = 6, 8, 10$ at zero temperature in Fig. 4(b). Using the condition $g^2(k_{\text{cr}}) = g_{\text{cr}}^2$, we can relate the solution of the β_{g^2} function near the fixed point to the scale k_{cr} , where the coupling g^2 exceeds its critical value g_{cr}^2 . The fact that k_{cr} sets the scale for the critical temperature T_{cr} finally yields the following relation for the critical temperature near N_f^{cr} [11]:

$$T_{\text{cr}} \sim k_0 |N_f - N_f^{\text{cr}}|^{-\frac{1}{\Theta}}, \quad (7)$$

where Θ should be evaluated at N_f^{cr} and the scale k_0 is implicitly defined by a suitable definition for the β_{g^2} function. Relation (7) is remarkable since it relates two *universal* quantities to each other: the shape of the phase boundary and the IR critical exponent Θ . The good agreement between the full numerical result for the phase boundary and the analytic result Eq. (7) around N_f^{cr} is shown in Fig. 4(a). This allows us to conclude that the symmetry status of the system for a large number of quark flavors is governed by the fixed-point regime where dimensionful scales such as Λ_{QCD} lose their importance.

4 Summary and Outlook

We have shown that the functional RG allows for a systematic and consistent expansion of QCD. Our truncation of the effective action based on an operator expansion seems to be promising for a study of QCD at zero and finite temperature, at least in the chirally symmetric regime. We have determined the chiral phase boundary of QCD in the plane of temperature and flavor number. Our quantitative results for small N_f are in agreement with lattice simulations for $N_f = 2, 3$. For large N_f we observe a flattening of the phase boundary near N_f^{cr} , owing to the IR fixed-point structure of QCD. Future extensions should include mesonic operators which can be treated with RG rebosonization techniques [38, 39]. We refer the reader to the lecture notes of H. Gies [19] for an introduction to such techniques. An extension of our present approach in this direction would not only provide access to the broken phase and mesonic properties, but also permit a study of the order of the phase transition.

The author would like to thank H. Gies for his collaboration on the work presented here, and is grateful to him and to B. Klein for proofreading the manuscript. The author acknowledges support from the GSI Darmstadt, from the DFG under contract Gi 328/1-3 (Emmy-Noether program) and from a fellowship provided by the organizers of the ECT* school.

References

1. Z. Fodor and S. D. Katz: JHEP **0203**, 014 (2002)
2. C. R. Allton, S. Ejiri, S. J. Hands, O. Kaczmarek, F. Karsch, E. Laermann and C. Schmidt: Phys. Rev. D **68**, 014507 (2003)
3. F. Karsch, E. Laermann and A. Peikert: Nucl. Phys. B **605** (2001) 579
4. F. J. Wegner and A. Houghton: Phys. Rev. A **8**, 401 (1973)
5. K. G. Wilson and J. B. Kogut: Phys. Rept. **12**, 75 (1974)
6. J. Polchinski: Nucl. Phys. B **231**, 269 (1984)
7. C. Wetterich: Phys. Lett. B **301** (1993) 90
8. T. R. Morris: Int. J. Mod. Phys. A **9**, 2411 (1994)
9. E. Shuryak: Prog. Part. Nucl. Phys. **53**, 273 (2004)
10. J. Braun and H. Gies: arXiv:hep-ph/0512085
11. J. Braun and H. Gies: JHEP **0606**, 024 (2006)
12. H. Gies: Phys. Rev. D **66**, 025006 (2002)
13. H. Gies: Phys. Rev. D **68**, 085015 (2003)
14. D. F. Litim and J. M. Pawłowski: Phys. Rev. D **66**, 025030 (2002)
15. M. Reuter and C. Wetterich: Nucl. Phys. B **417**, 181 (1994)
16. F. Freire, D. F. Litim and J. M. Pawłowski: Phys. Lett. B **495**, 256 (2000)
17. M. Reuter and C. Wetterich: Phys. Rev. D **56**, 7893 (1997)
18. U. Ellwanger: Phys. Lett. B **335** (1994) 364
19. H. Gies: arXiv: hep-ph/0611146, contribution to this volume (2006).
20. L. F. Abbott: Nucl. Phys. B **185**, 189 (1981)
21. N. K. Nielsen and P. Olesen: Nucl. Phys. B **144**, 376 (1978)

22. W. Dittrich and V. Schanbacher: Phys. Lett. B **100**, 415 (1981)
23. J. P. Blaizot, E. Iancu and A. Rebhan: Phys. Lett. B **470**, 181 (1999)
24. J. P. Blaizot, E. Iancu and A. Rebhan: Phys. Rev. D **63**, 065003 (2001)
25. L. von Smekal, R. Alkofer and A. Hauck: Phys. Rev. Lett. **79**, 3591 (1997)
26. J. M. Pawłowski, D. F. Litim, S. Nedelko and L. von Smekal: Phys. Rev. Lett. **93**, 152002 (2004)
27. C. S. Fischer and H. Gies: JHEP **0410**, 048 (2004)
28. T. Kugo and I. Ojima: Prog. Theor. Phys. Suppl. **66** (1979) 1
29. V. N. Gribov: Nucl. Phys. B **139**, 1 (1978)
30. S. Bethke: Nucl. Phys. Proc. Suppl. **135** (2004) 345
31. A. Maas, J. Wambach, B. Gruter and R. Alkofer: Eur. Phys. J. C **37**, 335 (2004)
32. H. Gies and J. Jaeckel: Phys. Rev. Lett. **93**, 110405 (2004)
33. H. Gies and J. Jaeckel: Eur. Phys. J. C **46**, 433 (2006)
34. H. Gies, J. Jaeckel and C. Wetterich: Phys. Rev. D **69** (2004) 105008
35. T. Banks and A. Zaks: Nucl. Phys. B **196**, 189 (1982)
36. V. A. Miransky and K. Yamawaki: Phys. Rev. D **55**, 5051 (1997)
37. T. Appelquist, J. Terning and L. C. R. Wijewardhana: Phys. Rev. Lett. **77**, 1214 (1996)
38. H. Gies and C. Wetterich: Phys. Rev. D **65** (2002) 065001
39. H. Gies and C. Wetterich: Phys. Rev. D **69**, 025001 (2004)